Brief Communication: Representation of heat conduction into the ice in marine ice shelf melt modelling

Jonathan Wiskandt[1,2] and Nicolas C. Jourdain[3]

[1]Department of Meteorology, Stockholm University, Stockholm, Sweden
[2]Bolin Centre for Climate Research, Stockholm, Sweden
[3]Univ. Grenoble Alpes/CNRS/IRD/G-INP/INRAE, IGE, Grenoble, France

Correspondence: Jonathan Wiskandt (jonathan.wiskandt@misu.su.se)

Abstract.

Basal melt of marine terminating glaciers is a key uncertainty in predicting the future climate and the evolution of the Antarctic and Greenland ice sheets. Regional ocean circulation models rely on an approximated heat budget at the ice–ocean interface that includes turbulent heat flux from the ocean below, latent heat for phase transition, and heat conduction into the ice, to parametrize melt rates. Here we review the formulations of Holland and Jenkins (1999) for the approximation of heat conduction into the ice, utilizing three distinct observed ice temperature profiles. We show that the formulation accounting for constant vertical advection and vertical diffusion of heat into the ice best represents the observed ice temperature profiles. Using idealised ocean simulations of a Greenlandic fjord and observed melt rates from Antarctica, we find a difference of up to 28% (average of 12%) in melt rate between the different approximations.

1 Introduction

In ocean general circulation models (OGCM), marine-terminating glaciers are usually assumed static and the local melt rate is parametrized using a set of three equations consisting of a linearization of the local freezing point temperature of water, as well as heat and salt budgets at the ice-ocean interface (Holland and Jenkins, 1999). The turbulent transport of heat from the water to the ice-ocean interface is partly balanced by the heat conduction into the ice. Any excess of heat from the combination of these two processes is used as latent heat for the solid to liquid phase change. Hence, a good representation of ice shelf basal melting in ocean models requires accurate simulations of both the turbulent heat transport in the water below the ice and the heat conduction into the ice shelf.

Heat conduction into the ice has often been neglected in ocean simulations resolving ice shelf cavities, with the idea that the resulting bias does not affect melt rates by more than 10% (Dinniman et al., 2016; Holland and Jenkins, 1999). Other models have adopted a crude representation of this flux, by assuming a linear temperature profile between the freezing temperature at ice shelf base and a typical annual mean air temperature at the ice shelf surface (e.g., Losch, 2008; Mathiot et al., 2017). More than 60 years ago, Wexler (1960) proposed a more elaborated formulation of this conductive heat flux by accounting for heat advection by the vertical ice motion, based on the observation of a few vertical temperature profiles. The formulation

was completed by Holland and Jenkins (1999) who proposed a linear approximation of Wexler's solution so that it can be incorporated in the solution of the three-equation system used to estimate basal melt rates in ocean models.

In this brief communication, we review these approaches and asses them using, for the first time, ice temperature profiles representing multiple typical scenarios of refreezing and melting. We further discuss the approaches' accuracies by applying them to realistic applications, and estimate the influence of heat conduction on ice shelf basal melt rates around Antarctica. Additionally, we investigate the relative importance of the heat conduction in the presence of a realistic ocean circulation and possible ice-ocean feedbacks. We propose future directions to improve the calculation of these fluxes in ocean or Earth system models.

2 Assessment of the various approaches

The heat budget at the ice–ocean interface that is used to derive melt rates in ocean models can be expressed as:

$$m\,L \;=\; \rho_{\mathrm{w}}\,c_{\mathrm{w}}\,u_{\star}\,\Gamma_{\mathrm{T}}\,(T_{\mathrm{w}} - T_{z_{\mathrm{d}}}) + \rho_{\mathrm{i}}\,c_{\mathrm{i}}\,\kappa_{\mathrm{i}}\left(\frac{\partial T_{\mathrm{i}}}{\partial z}\right)_{z_{\mathrm{d}}} \tag{1}$$

where m is the melt rate expressed in $\mathrm{kg\,m^{-2}\,s^{-1}}$ (negative in case of refreezing), ρ_{w} and ρ_{i} the densities of seawater and ice, L the melting/freezing latent heat of water, c_{w} and c_{i} the heat capacity of seawater and ice, $u_{\star}$ the friction velocity calculated by the ocean model, Γ_{T} the turbulent transfer parameter of temperature, κ_{i} the heat diffusivity of ice, T_{i} the ice temperature, T_{w} the ocean temperature at some distance from the ice–ocean interface, $T_{z_{\mathrm{d}}}$ the local freezing point temperature, and z_{d} the ice draft vertical position (z negative below sea level and increasing upward).

The three common approximations made in ocean models to deal with heat conduction in the ice are:

$$\begin{cases} \rho_{\mathrm{i}}\,\kappa_{\mathrm{i}}\left(\dfrac{\partial T_{\mathrm{i}}}{\partial z}\right)_{z_{\mathrm{d}}} = 0 & \text{(A)} \\[2ex] \rho_{\mathrm{i}}\,\kappa_{\mathrm{i}}\left(\dfrac{\partial T_{\mathrm{i}}}{\partial z}\right)_{z_{\mathrm{d}}} = \rho_{\mathrm{i}}\,\kappa_{\mathrm{i}}\,\dfrac{T_{\mathrm{s}} - T_{z_{\mathrm{d}}}}{z_{\mathrm{s}} - z_{\mathrm{d}}} & \text{(B)} \\[2ex] \rho_{\mathrm{i}}\,\kappa_{\mathrm{i}}\left(\dfrac{\partial T_{\mathrm{i}}}{\partial z}\right)_{z_{\mathrm{d}}} = (T_{\mathrm{s}} - T_{z_{\mathrm{d}}})\,\max\{m, 0\} & \text{(C)} \end{cases} \tag{2}$$

where T_{s} is the ice surface temperature at height z_{s}.

Approximation (A) in eq. (2) would be a good approximation if there were ice shelves close to the ocean freezing point over their entire thickness, but such ice shelves are likely unstable (Morris and Vaughan, 2003). It can still be a reasonable approximation for locations where ice shelves have a layer of marine ice at their base (Fig. 1a), although the permeable nature of this type of ice makes proper calculations complicated (Wang et al., 2022).

Approximation (B) in eq. (2) assumes no heat advected by the ice and a temperature profile that has reached a steady state between the freezing temperature at the base and a constant surface temperature. This seems to be a good approximation for the Ross Ice Shelf (RIS, Fig. 1b). The ice typically takes 1,000 years to go from the grounding line to the borehole of the

shown temperature profile (Mouginot et al., 2019), which corresponds to the typical time taken by heat to be conducted from the surface or the base to the middle of a 400 m thick ice shelf (estimated as $(H/2)^2/\kappa_\mathrm{i}$ where H is the ice thickness). The ice may take less than a century to cross some of the smaller ice shelves of similar thickness (Mouginot et al., 2019), which makes it unlikely that a thermal steady state is reached for these other ice shelves. Furthermore, Ross is characterized by very low basal melt rates (Rignot et al., 2013) and relatively low accumulation rate at the surface (Kittel et al., 2021), which is expected to result in relatively low ice vertical velocities. Therefore, the thermal regime is very different for small ice shelves with high melt rates, such as the Pine Island Ice Shelf, characterized by a strong temperature gradient at the base (Fig. 1c).

Approximation (C) in eq. (2) is made to account for vertical heat advection and was obtained by Holland and Jenkins (1999). They considered a vertical ice velocity directly proportional to the basal melt rate, i.e., they assumed that the melted ice was instantaneously compensated by surface accumulation or ice flow convergence, which is correct for a constant ice shelf shape. The formulation of eq. (2C) is a linearization of a more complex expression that tends to zero for refreezing rates greater than $\sim$0.1 meters of ice per year (Holland and Jenkins, 1999). This formulation represents both a uniform ice temperature gradient throughout the ice shelf thickness associated with weak melt (Fig. 1b), and strong ice temperature gradients at the ice shelf base associated with strong melt rates (Fig. 1c). Here, a steady state is still assumed, but the characteristic time to reach the steady state is imposed by the basal melt rate and not by heat conduction (See SI for a detailed discussion). The typical aspect ratio and horizontal ice velocities make this approximation reasonable for many ice shelves of Antarctica and Greenland (Rignot et al., 2013; Mouginot et al., 2019).

When considering the variety of ice temperature profiles found in Antarctica (Fig. 1a-c), it appears that approximation (A) only works in the presence of refreezing (Fig. 1a) while approximation (B) only works for large ice shelves with very weak basal melt rates (Fig. 1b). Approximation (C) appears as the only one able to represent the variety of temperature profiles. In case of refreezing ($m < 0$ in eq. (2C)), no heat is conducted into the ice (Fig. 2a), which is consistent with the vertical temperature profiles observed in the marine ice layer beneath the Amery Ice Shelf (Fig. 1a). In case of actual melting ($m > 0$ in eq. (2C)), the conductive heat flux is proportional to melt rates, consistent with the strong temperature gradients observed at the base of Pine Island ice shelf. The range of very weak melt rates ($-0.05 < m < 0.05$ m yr^{-1}) is the only one where the linear temperature profile is a better approximation than the linearization of Holland and Jenkins (Fig. 2a).

If we assume positive melt rates and use eq. (1), we can estimate the relative difference between approximation (A) compared to approximation (C):

$$\frac{\Delta m}{m} = \frac{c_\mathrm{i}\left(T_\mathrm{s} - T_{z_\mathrm{d}}\right)}{L} \tag{3}$$

Considering the parameter values used in Holland and Jenkins (1999), melt rates calculated without considering heat conduction in the ice are overestimated by 11% for a surface temperature of -20°C and a freezing point temperature of -2°C at the ice base. The overestimation is often similar when using the linear temperature profile rather than nothing, except in the absence of basal melting.

Applying eq. (3) to the observed melt rates in Antarctica gives an idea of where differences in the heat flux estimation have the largest effect on melt (Fig. 3). We use the 40-year (1980-2019) average snow surface temperatures as T_s and calculate

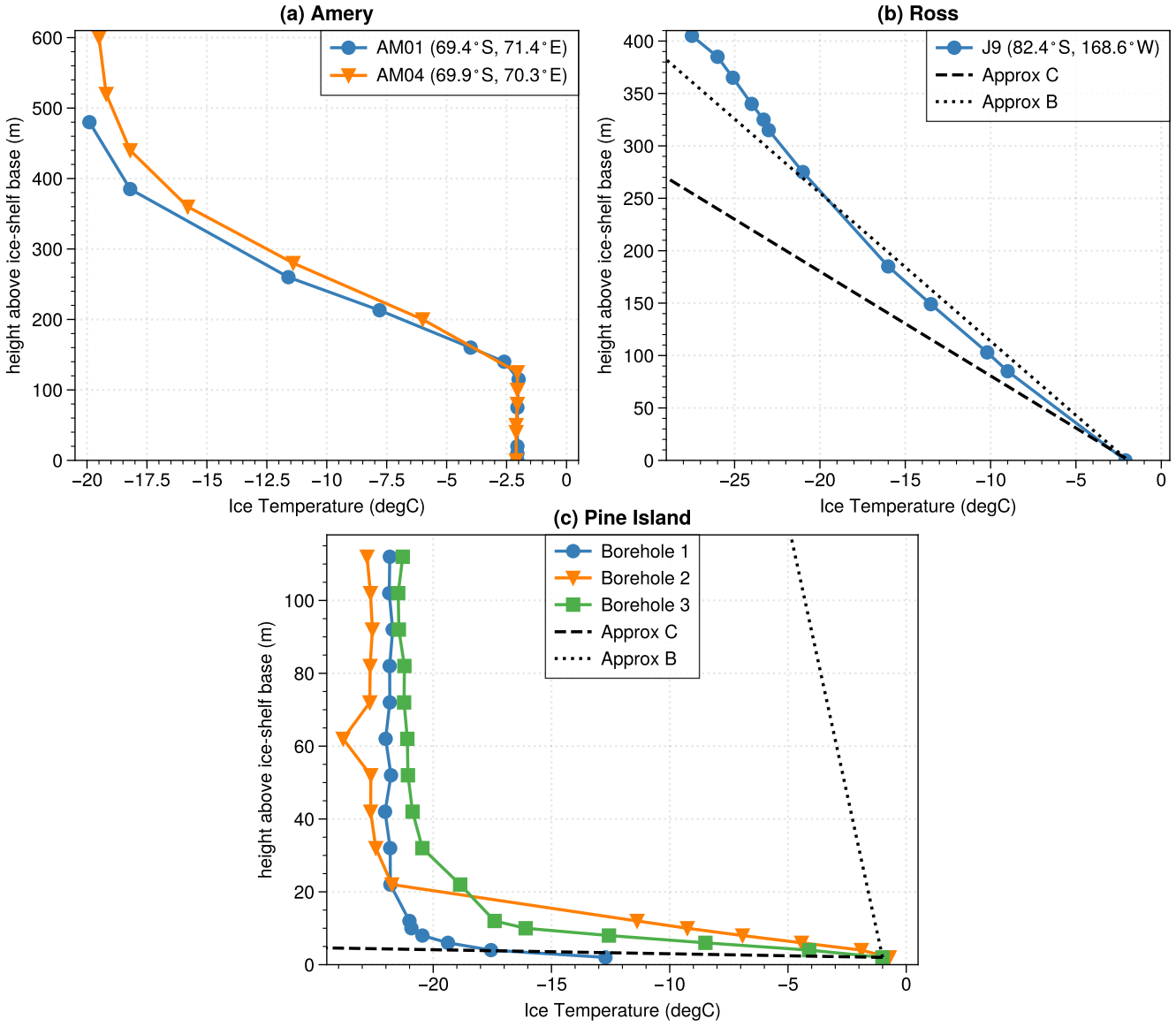

Figure 1. Ice temperature profiles measured by thermistor strings in boreholes at (a) two sites on Amery Ice Shelf (69.4°S, 71.4°E and 69.9°S, 70.3°E; referred to as AM01 and AM04, respectively) (b) one site in the middle of the Ross Ice Shelf (82.4°S, 168.6°W; referred to as J9), and (c) three sites on Pine Island Ice Shelf (75.1°S, 100.5°W). Black dashed and dotted lines in (b) and (c) show temperature profiles approximated from Eq. (2B) and (2C) using observed melt rates, annually averaged surface temperature. A layer of marine ice is present underneath the ice shelf at sites AM01 and AM04 (more than 100 m thick) and at site J9 (6 m thick).

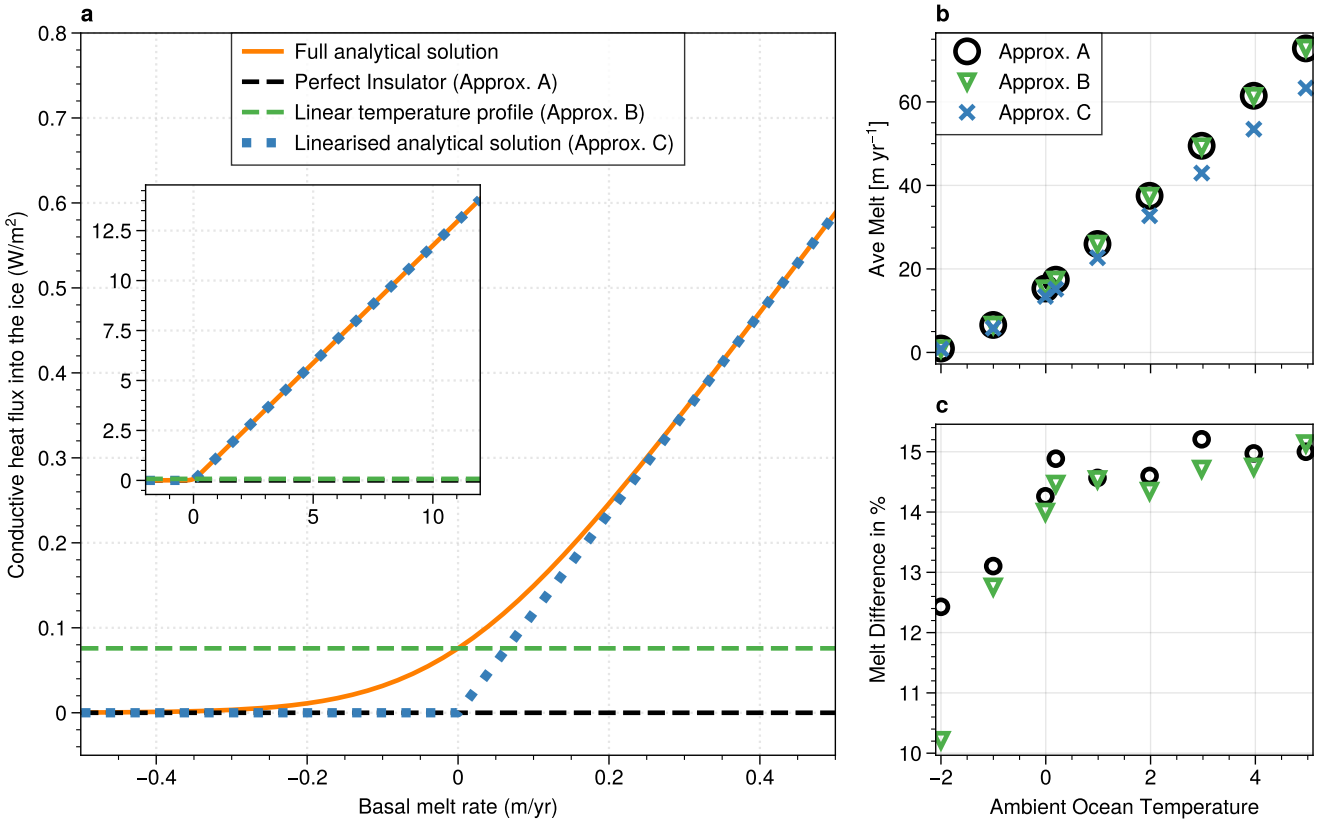

Figure 2. a) Conductive heat flux at the ice shelf base as a function of the basal melt rate expressed in meters of ice per year. The inset shows the same lines but with a broader range of melt rates. The blue line is the full analytical solution provided by Holland and Jenkins (1999), the dashed orange line is the linear simplification that they suggest (approximation C in eq. 2), and the green line is derived from the assumption of a linear temperature profile across the ice shelf thickness (approximation B in eq. 2). b) Simulated average melt rate from identical MITgcm ocean simulations using the three different approximations of eq. 2 as a function of bottom layer ocean Temperature. c) Melt rate difference with respect to approximation C.

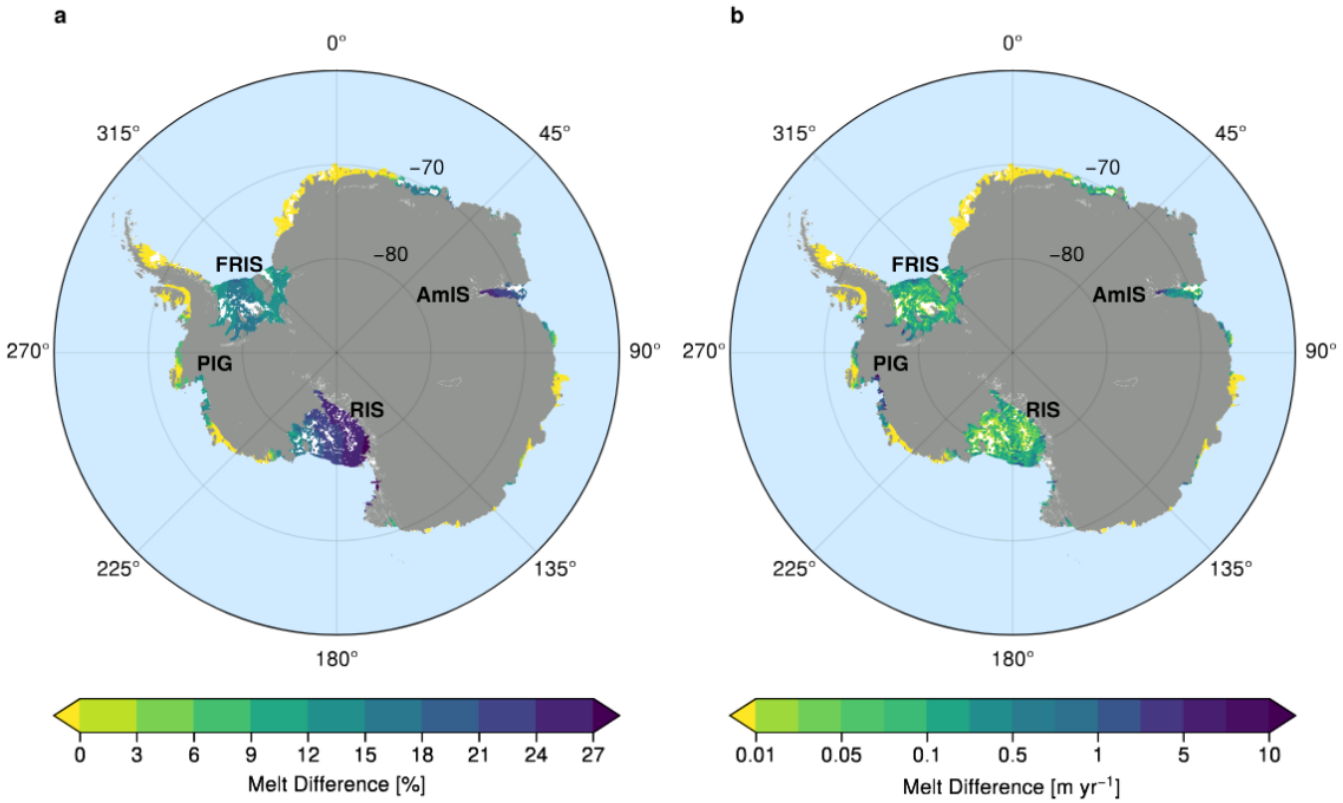

Figure 3. Map of Antarctica showing relative melt rate differences (Eq. 3) between Approximation (A) and (C) and respective absolute values when applied to melt rate data for floating ice shelves (b). White areas indicate regions of refreezing.

the pressure-dependent freezing point temperature T_{z_d} using a typical salinity of 34.6 g kg^{-1} everywhere. Ice shelves in the Amundsen embayment and the large ice shelves show a difference of around 12% with even higher values seen at Amery Ice Shelf (AmIS) and the eastern Ross Ice Shelf (RIS, both above 27%). In the most part of RIS this leads to only small differences in absolute numbers (below 0.1 m yr^{-1}, Fig. 3b), since melt rates here are very low (Rignot et al., 2013). In crucial areas, such as close to the grounding lines of Filchner-Ronne Ice Shelf (FRIS), most of AmIS and the smaller ice shelves draining towards the Amundsen Sea, the difference is multiple meters per year, surpassing even 10 m yr^{-1} at Pine Island Glacier and AmIS. At the calving fronts of FRIS and RIS melt rate differences are around 1 m yr^{-1}.

3 Application to ocean simulations of a small cavity

For a practical implementation of approximation (C) in an ocean model, the criterion on m to bound the heat conduction to zero is not very convenient, as this would require some iterations of the three-equation system because m is a solution that is not known a priori. A more practical solution is to check the sign of the thermal forcing ($T_\mathrm{w} - T_{z_\mathrm{d}}$ in eq. 1) to decide whether

or not heat conduction is set to zero. This is common procedure to implement the three equations in ocean modelling. We test this implementation in the MITgcm ocean model (Adcroft et al., 2004) and evaluate whether the relative importance of heat conduction, as derived from the theory, is still valid in the presence of a realistic ocean circulation and possible ice-ocean feedbacks.

To show the differences between the three approaches in the melt parametrization in a regional circulation model, we set up a suite of idealized, 2D, non–rotational simulations (Wiskandt et al., 2023) in MITgcm with varying ocean temperatures comparing the three different approaches introduced in eq. 2. The geometry is representative of a long and narrow fjord, typically found around Greenland. The domain is 30 km long and 1 km deep with an ice shelf covering the first 20 km of the domain with a grounding line depth of 950 m and a 50 m deep vertical front. Note that none of the present simulations exhibits refreezing. For all details of the simulation refer to Wiskandt et al. (2023).

Given the constant small difference between the conductive heat fluxes from approximation (A) and (B) (Fig. 2a), simulated melt rates are very similar in these two approximations (Fig. 2b-c). The differences in absolute melt rate are barely discernible by eye, and relative differences show a difference of $<1\%$ for the simulated temperature range, except for the coldest experiment (Fig. 2c). The difference between approximation (C) and either (A) or (B) is between 10-15% in most experiments, i.e. those with temperature $\geq 0°C$ show a difference of 14-15%.

4 Conclusions

Former ocean circulation studies at both Greenlandic and Antarctic marine-terminating glaciers implemented approximation (A) (e.g. Gwyther et al., 2020; Comeau et al., 2022) or (B) (e.g. De Rydt and Naughten, 2024; Wiskandt et al., 2023; Holland et al., 2008; Losch, 2008) in eq. 2 for heat conduction into the ice. Combining for the first time a suite of ice temperature profiles representing a variety of melting conditions, we have shown that only approximation (C) estimates the temperature gradient in the ice accurately across the full range of possible melting and refreezing scenarios. We provide a novel map of the local impact of heat conduction parametrization on melt rates in Antarctica and find that Approximations (A) and (B) overestimate melt rates by up to 25% (12% average) compared to approximation (C).

We have shown that an inaccurate representation of heat conduction into the ice induces biases in melt rates with a high spatial variability. This cannot be corrected by tuning a constant drag or heat transfer coefficient as often done in ocean models. Accurate local melt rates are also crucial to estimate the stability of the ice shelf, e.g., close to the grounding line, where changes in ice shelf geometry can trigger rapid ice loss (De Rydt and Naughten, 2024). In ocean circulation models, a melt-dependent local temperature gradient is relatively straightforward to implement and, in fact, available in MITgcm in the SHELFICE package (Losch, 2008). The Finite-volumE Sea ice–Ocean Model (FESOM2) (Danilov et al., 2017) also uses an approach similar to approximation (C).

We argue here, that the parameterization using a linear dependency of the heat flux on the melt rate is the most accurate; it is nonetheless based on several approximations (Holland and Jenkins, 1999). To accurately model the ice-ocean interactions, a coupled ice-sheet–ocean model should be used, with a representation of both vertical and lateral heat conduction and heat

advection in the ice (Sergienko et al., 2013). A large part of the current ice-sheet models however, do not explicitly simulate the ice-sheet temperatures and sometimes use approximations of the Stokes equation that prevent a good representation of vertical heat advection in ice. Hence, we suggest that coupled models currently under development should consider calculating the ice sheet temperature gradients or heat fluxes and transfer them into the ocean model to accurately calculate the melt rate using the three-equation system. For non–coupled models the authors strongly suggest to implement approach (C) of eq. 2 when parameterizing marine basal melt, as it more accurately represents the heat conduction into the ice and comes at very little additional computational cost.

Code and data availability. The configuration files necessary to reproduce the simulations used in the present study employed the MITgcm (downloaded in 2020 from https://github.com/MITgcm/MITgcm/releases/tag/checkpoint67s, last access: 4 July 2023), and are/will be available through the Bolin Research Centre Data Centre (https://git.bolin.su.se/jowi1379/IceShelf_HeatFlux_Code/). Also available there are/will be time averaged fields and key diagnostics from the simulations and code needed to reproduce the shown figures. See SI for a detailed account of all data used.

Author contributions. JW and NCJ initiated this work and reviewed the theory together. JW ran the MITgcm simulations and analysed the results. All authors discussed the results and contributed to the manuscript.

Competing interests. Nicolas Jourdain is an editor of The Cryosphere.

Acknowledgements. NCJ's contribution was supported by the European Union's Horizon 2020 research and innovation programme (EU-H2020) under grant agreement No 101003536 (ESM2025), and by the Agence Nationale de la Recherche - France 2030 as part of the PEPR TRACCS programme under grant number ANR-22-EXTR-0010. JW's work was performed within a pair PhD project funded by the Faculty of Science, Stockholm University, and granted to the Department of Mathematics, division of Computational Mathematics, and the Department of Meteorology (SUFV-1.2.1-0124-17). The MITgcm simulations were enabled by resources provided by the National Academic Infrastructure for Supercomputing in Sweden (NAISS) at the National Supercomputer Centre (NSC), partially funded by the Swedish Research Council through grant agreements no. 2022-06725.

References

Adcroft, A. J., Hill, C., Campin, J. M., Marshall, J., and Heimbach, P.: Overview of the formulation and numerics of the MIT GCM, in: Proceedings of the ECMWF seminar series on Numerical Methods, Recent developments in numerical methods for atmosphere and ocean modelling, pp. 139–149, ECMWF, URL: https://www.ecmwf.int/en/elibrary/7642-overview-formulation-and-numerics-mit-gcm, 2004.

Comeau, D., Asay-Davis, X. S., Begeman, C. B., Hoffman, M. J., Lin, W., Petersen, M. R., Price, S. F., Roberts, A. F., Van Roekel, L. P., Veneziani, M., et al.: The DOE E3SM v1.2 cryosphere configuration: Description and simulated Antarctic ice-shelf basal melting, Journal of Advances in Modeling Earth Systems, 14, e2021MS002 468, 2022.

Danilov, S., Sidorenko, D., Wang, Q., and Jung, T.: The Finite-volumE Sea ice–Ocean Model (FESOM2), Geoscientific Model Development, 10, 765–789, https://doi.org/10.5194/gmd-10-765-2017, 2017.

De Rydt, J. and Naughten, K.: Geometric amplification and suppression of ice-shelf basal melt in West Antarctica, The Cryosphere, 18, 1863–1888, https://doi.org/10.5194/tc-18-1863-2024, 2024.

Dinniman, M. S., Asay-Davis, X. S., Galton-Fenzi, B. K., Holland, P. R., Jenkins, A., and Timmermann, R.: Modeling ice shelf/ocean interaction in Antarctica: A review, Oceanography, 29, 144–153, 2016.

Gwyther, D. E., Kusahara, K., Asay-Davis, X. S., Dinniman, M. S., and Galton-Fenzi, B. K.: Vertical processes and resolution impact ice shelf basal melting: A multi-model study, Ocean Modelling, 147, 101 569, https://doi.org/10.1016/j.ocemod.2020.101569, publisher: Elsevier Ltd., 2020.

Holland, D. M. and Jenkins, A.: Modeling thermodynamic ice-ocean interactions at the base of an ice shelf, Journal of Physical Oceanography, 29, 1787–1800, https://doi.org/10.1175/1520-0485(1999)029<1787:mtioia>2.0.co;2, 1999.

Holland, P. R., Jenkins, A., and Holland, D. M.: The response of Ice shelf basal melting to variations in ocean temperature, Journal of Climate, 21, 2558–2572, https://doi.org/10.1175/2007JCLI1909.1, 2008.

Kittel, C., Amory, C., Agosta, C., Jourdain, N. C., Hofer, S., Delhasse, A., Doutreloup, S., Huot, P.-V., Lang, C., Fichefet, T., and Fettweis, X.: Diverging future surface mass balance between the Antarctic ice shelves and grounded ice sheet, The Cryosphere, 15, 1215–1236, https://doi.org/10.5194/tc-15-1215-2021, 2021.

Losch, M.: Modeling ice shelf cavities in a z coordinate ocean general circulation model, Journal of Geophysical Research: Oceans, 113, 1–15, https://doi.org/10.1029/2007JC004368, 2008.

Mathiot, P., Jenkins, A., Harris, C., and Madec, G.: Explicit representation and parametrised impacts of under ice shelf seas in the z_* coordinate ocean model NEMO 3.6, Geoscientific Model Development, 10, 2849–2874, 2017.

Morris, E. M. and Vaughan, D. G.: Spatial and temporal variation of surface temperature on the Antarctic Peninsula and the limit of viability of ice shelves, Antarctic Research Series, 79, 2003.

Mouginot, J., Rignot, E., and Scheuchl, B.: Continent-wide, interferometric SAR phase, mapping of Antarctic ice velocity, Geophysical Research Letters, 46, 9710–9718, 2019.

Rignot, E., Jacobs, S., Mouginot, J., and Scheuchl, B.: Ice-shelf melting around Antarctica, Science, 341, 266–270, 2013.

Sergienko, O. V., Goldberg, D. N., and Little, C. M.: Alternative ice shelf equilibria determined by ocean environment, Journal of Geophysical Research: Earth Surface, 118, 970–981, https://doi.org/10.1002/jgrf.20054, 2013.

Wang, Y., Zhao, C., Gladstone, R., Galton-Fenzi, B., and Warner, R.: Thermal structure of the Amery Ice Shelf from borehole observations and simulations, The Cryosphere, 16, 1221–1245, 2022.

Wexler, H.: Heating and melting of floating ice shelves, Journal of Glaciology, 3, 626–645, 1960.

Wiskandt, J., Koszalka, I. M., and Nilsson, J.: Basal melt rates and ocean circulation under the Ryder Glacier ice tongue and their response to climate warming: a high-resolution modelling study, The Cryosphere, 17, 2755–2777, https://doi.org/10.5194/tc-17-2755-2023, 2023.